SYNTHESIS AND CHARACTERIZATION OF PLASMONIC-ASSISTED PHOTODETECTION PERFORMANCE BASED ON POROUS SILICON

SHIREEN MOHAMMED ABED

UNIVERSITI SAINS MALAYSIA

2025

SYNTHESIS AND CHARACTERIZATION OF PLASMONIC-ASSISTED PHOTODETECTION PERFORMANCE BASED ON POROUS SILICON

by

SHIREEN MOHAMMED ABED

Thesis submitted in fulfilment of the requirements
for the degree of
Doctor of Philosophy

February 2025

ACKNOWLEDGEMENT

First and foremost, I am profoundly grateful to Almighty Allah for blessing me with health, patience, and inspiration throughout this research.

I am deeply thankful to my main supervisor Dr. Sabah M. Mohammad, for his exceptional academic guidance and intellectual support throughout my PhD studies. His mentorship has been instrumental in shaping this work, and I am deeply appreciative of his unwavering presence and guidance throughout this academic journey

I am also very grateful to my co-supervisor, Professor Dr Zainuriah Binti Hassan, for her invaluable guidance and encouragement during challenging times. Her unwavering support has been crucial throughout my PhD journey.

This thesis is dedicated to my father, mother, brothers, and sisters, whose prayers, encouragement, and steadfast support have strengthened my research.

I would like to thank the University of Anbar for enabling me to pursue my PhD at Universiti Sains Malaysia. I also thank the Nano-Optoelectronics Research and Technology Laboratory (NOR Lab) staff for their technical assistance during my laboratory work.

Shireen Mohammed Abed
Penang, Malaysia. 2025

.

TABLE OF CONTENTS

LIST OF TABLES

Page

LIST OF FIGURES

Page

LIST OF SYMBOLS

a	Absorption coefficient
A, b & c	Lattice constants
a_0, C_0	Lattice constants at 270C
Ag	Silver
Ar	argon
Au	Gold
Br_2	Bromine
C	carbon
Cu	copper
d	Interplanar spacing between the planes in the atomic lattice
D	Average crystallite size
EQE	External Quantum Efficiency
F	fluorine
F(R)	Kubelka Munk function
Ge	germanium
h	Planck's constant
H_2	hydrogen gas
hkl	Miller indices
I_2	Iodine
I_{dark}	Dark current
I_{ph}	Photocurrent
I_{UV}/I_{DLE}	Ratio of the intensity of UV emission to the visible deep level emission
k	Scherrer constant
N_2	nitrogen gas

NaCl	Sodium chloride
Ni	nickel
O	oxygen
O^{2-}	oxygen ion
OH-	hydroxyl ions
O_i	interstitial oxygen
Pb	lead
R	responsivity
S	sensitivity
Si	silicon
Sn	tin
V_O	Oxygen vacancies
V_{Zn}	Zinc vacancies
Zn	zinc
Zn^{2+}	Zinc (II) ion
Zni	Zinc interstitial
ε_{zz}	The strain of the thin film
Θ	Bragg diffraction angle
λ	Wavelength
Eg	Energy bandgap

LIST OF ABBREVIATIONS

1D, 2D	One-dimensional, two-dimensional
ALAM	Atomic-layer additive manufacturing
ALD	Atomic layer deposition
AsF_5	Arsenic pentafluoride
CB	Conduction band
CBD	Chemical bath deposition
CSD	Chemical solution deposition
CVD	Chemical vapor deposition
DC	Direct current
DI	Deionized water
DLE	Deep-level emissions
EDS	The energy dispersive spectroscopy
EDX	The energy-dispersive X-ray
e-h	Electron-hole pairs
FTO	Fluorine-doped tin oxide
FWHM	Full width at half maximum
HCl	Hydrochloric acid
HEL	Extraction injection layer
HF	Hydrofluoric acid
HIL	Hole injection layer
HMT	Hexamethylenetetramine
IR	Infrared
ITO	Indium tin oxide
I–V	Current-Voltage
LDs	Laser diodes

LEDs	Light-emitting diodes
LSPR	Localized surface plasmon resonance
M	Metal
M^+	Metal ion
MBE	Molecular beam epitaxy
MCB-HM	Modified chemical bath-hydrothermal method
MOCVD	Metal-organic chemical vapour deposition
m-PSi	Macroporous silicon
MSM	Metal-semiconductor-metal
NaOH	Sodium hydroxide
NBE	Near band emission
NCs	Nanocomposite
NPs	Gold nanoparticles
NRs	Nanorods
OLEDs	Organic light-emitting diodes
OSCs	Organic solar cells
PANi	Polyaniline
PD	Photodetector
PEDOT: PSS	Poly(3,4-ethylenedioxythiophene): poly (styrene sulfonate)
PES	Polyethersulfone
PL	Photoluminescence
PLD	Pulsed laser deposition
PPy	Polypyrrole
PSi	Porous silicon
PVD	Vacuum deposition
RF	Radio frequency
RMS	Root mean square

RT	Room temperature
SBH	Schottky barrier height
SEM	Scanning electron microscopy
Si NWs	Silicon nanowires
SiF_4	Silicon tetrafluoride
SPR	Surface plasmon resonance
SPs	Surface plasmons
TEM	Transmission electron microscopy
TiO_2	Titanium dioxide
TM	Transverse magnetic
UV	Ultraviolet
UV-Vis	Ultraviolet–visible
VADCM	Vibration-assisted drop-cast method
VB	Valence band
XRD	The X-ray diffraction
ZAD	Zinc acetate dihydrate
ZnO	Zinc oxide
Φ_B	The schottky barrier height
Φ_m	Metal work function
Φs	Semiconductor work function
PV	Photovoltaic

SINTESIS DAN PENCIRIAN PRESTASI PENGESANAN FOTO BERBANTUKAN-PLASMONIK BERASASKAN SILIKON BERLIANG

ABSTRAK

Tesis ini menyelidiki sintesis dan pencirian pengesan foto logam-semikonduktor-logam (MSM) dan heterosimpangan p-n hibrid organik-tak organik berasaskan nanozarah (NPs) logam mulia berbantukan-plasmonik dan menggunakan substrat silikon berliang (PSi) yang menggunakan kaedah mudah dan kos-rendah untuk meningkatkan prestasi pengesanan foto merentas spektrum ultraungu-cahaya nampak-inframerah dekat (UV-Vis-NIR). Pertama, PSi telah difabrikasikan pada silikon biasa menggunakan punaran fotoelektrokimia. Substrat PSi yang terhasil menunjukkan keliangan yang tinggi, dengan diameter liang antara 199 hingga 750 nm, purata panjang liang 3.6 μm, dan nilai kekasaran punca min kuasa dua (RMS) adalah 70 nm. Imej mikroskopi imbasan elektron pancaran medan (FESEM) mendedahkan bahawa benih zink oksida (ZnO) yang dimendapkan dengan kaedah kos-rendah penuangan-titisan berbantukan-getaran (VADCM) atas PSi secara berkesan menyusup ke dalam liang dan melekat pada dinding dalaman, yang membawa kepada pertumbuhan nanorod (NRs) ZnO dengan kaedah hidroterma diubah suai di dalam liang dalam arah yang berbeza dan bilangan sambungan titik sentuhan yang lebih ketara antara rod, manakala yang dimendapkan oleh percikan frekuensi radio (RF) terkumpul di permukaan, yang membawa kepada pertumbuhan hidroterma NRs ZnO sebagai lapisan atas substrat PSi. Oleh itu, pengesan foto NR MSM-ZnO berprestasi lebih baik apabila ZnO dimendapkan atas substrat PSi menggunakan VADCM. Ia mencapai penambahan sebanyak 7.4, responsiviti (R) sebanyak 1.12 A/W, kecekapan kuantum luaran (EQE) sebanyak 372%, dan fotosensitiviti (S) sebanyak 645.5% di

bawah pencahayaan UV pada 375 nm pada voltan pincang 3 V. NPs sfera emas (Au) dan perak (Ag) dengan saiz purata 10.5 nm dan 31.5 nm, masing-masing, telah disintesis menggunakan kaedah ablasi denyutan laser dalam cecair (PLAL). NPs logam mulia ini dimendapkankan pada substrat ZnO NRs/PSi melalui pemendapan UV. Pengesan foto MSM berasaskan taburan NPs ZnO dengan campuran NPs logam mulia, terutamanya apabila menggunakan gabungan logam mulia yang berbeza, boleh meningkatkan responsiviti dengan ketara dalam julat panjang gelombang yang luas dan akhirnya meningkatkan prestasi keseluruhannya. R dan EQE pengesan foto MSM berasaskan taburan NRs ZnO dengan campuran NPs Au dan Ag dipertingkatkan hampir dua kali ganda berbanding pengesan foto berasaskan taburan NRs ZnO dengan sama ada NPs Au atau NPs Ag dan sekitar 21 kali ganda untuk R dan 25 kali untuk EQE berbanding peranti yang berasaskan NRs ZnO dengan tiada taburan NPs di bawah cahaya panjang gelombang 635 nm pada voltan pincang yang dikenakan sebanyak 4V. Selain itu, plasmonik campuran NPs Au dan Ag membantu peranti dalam mencapai nilai tertinggi S merentas semua panjang gelombang terpilih pada voltan pincang antara 0V hingga 3V, terutamanya pada yang berkuasa-sendiri, ia menunjukkan nilai S yang lebih tinggi sebanyak 248,900 %, 339,614%, 365,775%, 365,775%, 299,252% dan 232,166% masing-masing di bawah pencahayaan panjang gelombang 365 nm, 425 nm, 515 nm, 635 nm, 850 nm dan 940 nm. Pengesan foto heterosimpangan p-n yang difabrikasikan, yang terdiri daripada bahan hibrid organik-tak organik, menggabungkan NPs Au dan Ag yang tertanam dalam nanokomposit (NCs) poli(3,4-etilenadioksitiofen) poli (stirena sulfonat) (PEDOT:PSS) yang dimendapkan atas substrat PSi jenis-n menggunakan teknik senapang tuangan-udara panas. Mereka secara amnya menunjukkan tindak balas yang berfungsi dan mengesan panjang gelombang antara UV hingga IR dekat, terutamanya struktur peranti

berdasarkan gabungan NPs Au dan Ag yang tertanam dalam PEDOT:PSS mempamerkan nilai R, EQE dan S yang jauh lebih tinggi daripada peranti PEDOT:PSS tulen dalam julat 425-940 nm. Prestasi yang dipertingkatkan ini boleh dikaitkan dengan kesan hibrid resonans plasmon permukaan setempat (LSPR) yang timbul daripada interaksi sinergistik antara dua jenis nanozarah logam mulia. Walau bagaimanapun, peranti (Au:Ag) NPs:PEDOT:PSS)/PSi mencapai sensitiviti nilai tertinggi pada pincang sifar, mencapai 60,373%, 249,005%, 100,645% dan 957,268% masing-masing di bawah pencahayaan 365 nm, 635 nm, 850 nm dan 940 nm. Peranti (Au NPs: PEDOT:PSS)/PSi mempamerkan sensitiviti puncak masing-masing sebanyak 48,110% dan 85,900% pada 425 nm dan 515 nm.

SYNTHESIS AND CHARACTERIZATION OF PLASMONIC-ASSISTED PHOTODETECTION PERFORMANCE BASED ON POROUS SILICON

ABSTRACT

This thesis investigates the synthesis and characterization of metal-semiconductor-metal (MSM) and p-n heterojunction organic-inorganic hybrid photodetectors based on the noble metal nanoparticles (NPs) plasmonic-assisted and utilizing porous silicon (PSi) substrates using a simple and low-cost method to enhance photodetection performance across the ultraviolet-visible-near infrared (UV-Vis-NIR) spectrum. First, PSi were fabricated on bare silicon using photoelectrochemical etching. The resulting PSi substrate demonstrated high porosity, with pore diameters ranging from 199 to 750 nm, an average pore length of 3.6 μm, and a root mean square (RMS) roughness value of 70 nm. Field electron scanning electron microscopy (FESEM) images revealed that zinc oxide (ZnO) seeds deposited using the low-cost vibration-assisted drop-casting method (VADCM) on PSi effectively infiltrated the pores and adhered to the inner walls, which led to the growth of the ZnO nanorods (NRs) by modified hydrothermal method inside the pores in different directions and a more significant number of contact point connections between rods, whereas those deposited by radio frequency (RF) sputtering accumulated on the surface, which led to the hydrothermal growth of the ZnO NRs as a layer on the PSi substrate. Therefore, the MSM-ZnO NR photodetector performs better when ZnO is deposited on PSi substrate using VADCM. It achieved a gain of 7.4, a responsivity (R) of 1.12 A/W, an external quantum efficiency (EQE) of 372%, and photosensitivity (S) of 645.5% under UV illumination at 375 nm at a bias voltage of 3 V. Spherical gold (Au) and silver (Ag) NPs with average sizes of 10.5 nm and 31.5 nm, respectively, were synthesized using

the pulse laser ablation in liquid (PLAL) method. These noble metal NPs were deposited onto ZnO NRs/PSi substrates through UV photodeposition. MSM photodetectors based on the decoration of ZnO NRs with noble metal NPs, especially when employing a combination of different noble metals, can significantly improve their responsiveness over a broad range of wavelengths and ultimately enhance their overall performance. The R and EQE of the MSM photodetector based on the decoration of ZnO NRs with the mixture of Au and Ag NPs are improved by nearly two times over the photodetectors based on the decoration of ZnO NRs with either Au NPs or Ag NPs and around 21 times for R and 25 times for EQE over the device which based on the ZnO NRs with an absent decoration of the NPs under light of wavelength of 635 nm at applied bias voltage of 4V. Additionally, the plasmonic of a mixture of Au and Ag NPs assists the device in achieving the highest values of S across all selected wavelengths at bias voltages ranging from 0V to 3V, especially at self-powered, it demonstrates higher S values of 248,900 %, 339,614%, 365,775%, 365,775%, 299,252%, and 232,166% under illumination of wavelengths of 365 nm, 425 nm, 515 nm, 635 nm, 850 nm, and 940 nm respectively. The fabricated p-n heterojunction photodetectors, which consist of organic-inorganic hybrid materials, incorporate Au and Ag NPs embedded in poly(3,4-ethylenedioxythiophene) poly (styrene sulfonate) (PEDOT: PSS) nanocomposite (NCs) deposited on n-type PSi substrates using the casting-hot air gun technique. They generally demonstrated a functional response and detected wavelengths ranging from UV to near IR, mainly the device structure based on a combination of Au and Ag NPs embedded in PEDOT:PSS exhibited significantly higher values of the R, EQE and S than the device with pure PEDOT:PSS in the 425-940 nm range. This enhanced performance can be attributed to the hybrid localized surface plasmon resonance (LSPR) effect arising from the

synergistic interaction between the two types of noble metal nanoparticles. However, the (Au:Ag) NPs: PEDOT:PSS)/PSi device achieved the highest value sensitivity at zero bias, reaching 60,373%, 249,005%, 100,645%, and 957,268% under 365 nm, 635 nm, 850 nm, and 940 nm illumination, respectively. The (Au NPs: PEDOT: PSS)/PSi device exhibited peak sensitivities of 48,110%, and 85,900% at 425 nm and 515 nm, respectively.

CHAPTER 1

INTRODUCTION

1.1 General Introduction

Ultraviolet photodetectors (PDs), including Schottky photodiodes, metal-semiconductor-metal (MSM) PD structures, and p-n junction photodiodes, are crucial in detecting UV radiation. Their straightforward designs and rapid response capabilities contribute significantly to their overall efficiency [1]. MSM PDs, characterized by a high Schottky barrier, exhibit low leakage current and high breakdown voltage.

The application of thermal treatment significantly enhances the photoresponsivity and improves the photocurrent-to-dark current ratio in MSM PDs [2]. These devices are particularly preferred for UV detection due to their low capacitance per unit area, rapid response speed, minimal dark current, and ability to operate without an external bias. Similarly, p-n junction photodiodes offer fast response times, low dark current, and zero-bias operation capability.

Zinc oxide (ZnO), a semiconductor material is of significant interest owing to its distinctive characteristics. It possesses a broad direct energy gap of 3.37 eV, which contributes to high transparency within the visible spectrum, and exhibits a large exciton binding energy of approximately 60 meV, which provides high luminous efficiency at room temperatures. The thermal and chemical stability of ZnO, coupled with its excellent radiation resistance and high sensitivity to adsorbed oxygen make it suitable for harsh environments and various sensing technologies. In addition, ZnO is an inexpensive and non-toxic material that is ideal for applications in the ultraviolet

(UV) wavelength regions, highlighting its potential for diverse scientific and industrial applications [3, 4].

One-dimensional (1D) ZnO nanostructures are highly valued for their significant surface-to-volume ratio, distinct crystalline orientation, rapid response characteristics, exceptional sensitivity to UV light sensitivity, high concentration of surface trap states, and outstanding optical gain properties. These properties make 1D ZnO nanostructures, rendering them highly suitable for various applications, including laser diodes, gas sensors, light-emitting diodes (LEDs), solar cells, and UV photodetectors (PDs) [5, 6].

Porous silicon (PSi) is characterized by its adjustable roughness and strong absorbability properties [7, 8]. PSi supports integrating PSi-based optical devices [9]. The large surface area, open structure, and unique optical and electrical attributes of PSi play a critical role [10]. Diminishing the lattice constants of Si also contributes to alleviating the lattice mismatches that occur between ZnO and Si substrates [11].

Recently, PSi has proven a practical template for epitaxial regrowth, reducing structural defects and enabling the growth of high-quality, defect-free ZnO layers [12]. The material was discovered by accident in the mid-1950s by Arthur and Ingeborg Uhlir at Bell Laboratories [13].

Notably, PSi exhibits photoluminescence and electroluminescence characteristics close to those of direct bandgap semiconductors [14]. It is suitable for display technologies, optoelectronics, micromechanics, and biomedicine, with its characteristics defined by porosity, thickness, surface properties, and pore morphology [15-17].

The selection of seed material plays a vital role in successfully fabricating excellent and quality ZnO nanorods (NRs), influencing their size and growth characteristics. A smooth seed layer is necessary to mitigate the lattice mismatches on Si wafers, which facilitates the development of vertically aligned NRs with minimal defect densities.

Various methods such as magnetron sputtering, spray pyrolysis, pulsed laser deposition (PLD), and drop-casting of zinc (Zn) acetate mixture have been employed to fabricate c-axis textured ZnO seed layers. Among these techniques, drop-casting stands out for its simplicity and minimal equipment requirements. A study by Greene et al.[18] demonstrated that the thermal degradation of Zn acetate dihydrate in ethanol results in the formation of c-axis-oriented ZnO nanocrystalline layers on various substrates.

Numerous approaches have been utilized for synthesizing one-dimensional (1D) ZnO nanomaterials, such as plasma-enhanced chemical vapor deposition (PECVD) [19], electrochemical deposition (ECD), metal-organic chemical vapor deposition (MOCVD) [20], chemical vapor transport (CVT), condensation, molecular beam epitaxy (MBE) [21], pulsed laser deposition (PLD) [22], and the hydrothermal method [23].

Among these, the hydrothermal method is particularly notable for its low cost, ease of use, large-area deposition capability, low-temperature process, and environmental friendliness [24, 25]. This method produces high-quality crystalline films or powders with controlled size distribution and high purity, often without requiring high-temperature heat treatment [26, 27].

However, the defects on ZnO NRs surfaces from solution methods can cause detrimental defect-related emissions, impacting device responsiveness. Suppressing these deep-level emissions and enhancing UV emissions are essential for improving ZnO NR-based photodetector performance. To solve these challenges, recent studies have concentrated on the decoration of ZnO NRs with metal nanoparticles (NPs) such as gold (Au) [28, 29], silver (Ag) [30], and the mixture of (Au: Ag) NPs. This strategy utilizes the localized surface plasmon resonance (LSPR) phenomenon to passivate defect emissions and enhance photoresponse.

The LSPR effect enhances light interaction through various mechanisms, such as electric field improvement, hot electron creation, and thermo-plasmonic influences. This increased light interaction boosts the efficiency of photodetectors and photovoltaic devices [31]. The photodetector response is closely linked to the SPR resonance peak of the nanoparticles; when the SPR peak aligns with the UV detection range, it significantly enhances light absorption and the overall photoresponse. Furthermore, this approach provides a viable solution to the low photosensitivity problem in traditional ZnO-based devices.

Broadband PDs that are sensitive across the UV to infrared IR spectrum have garnered significant attention due to their potential applications in communications, video imaging, environmental monitoring, remote sensing, and biomedical detecting [32, 33]. These photodetectors demonstrate notable capabilities, including reliable operational stability, excellent detection efficiency, a compact design, rapid response times, and cost-effective manufacturing features that make them strong contenders for commercialization.

Researchers have increasingly focused on developing advanced broadband photodetectors using hybrid organic-inorganic structures [34]. These hybrid materials combine the beneficial attributes of organic and inorganic components.

Organic polymers like poly(3-hexylthiophene) (P3HT) and poly(3,4-ethylenedioxythiophene) poly(styrene sulfonate) (PEDOT: PSS) are widely used in photodetectors and solar cells for their outstanding performance [35]. PEDOT: PSS, in particular, is notable for its moderate bandgap, high electrical conductivity, and broad optical absorption extending into the infrared region. Research has shown that hybrid photodetectors incorporating PEDOT: PSS with n-type inorganic semiconductors exhibit promising photoresponse characteristics, highlighting their potential for advanced photodetection applications [36].

1.2 Problem Statement

This thesis addresses several critical issues, which can be summarized as follows: the seed material is crucial in the formation of high-quality ZnO (NRs), as it significantly affects the dimensions of the growing ZnO NRs [37]. For the effective growth of ZnO nanorods on a Si wafer, a uniform seed layer is essential to address the lattice mismatch between ZnO and Si [38]. A properly maintained seed layer is necessary to achieve vertically oriented nanorods with minimal defects [39].

In recent developments, c-axis textured ZnO seed layers have been produced using several deposition methods, such as spray pyrolysis, PLD, magnetron sputtering, and the thermal decomposition of zinc acetate mixture applied via drop-casting techniques [40].

Among these methods, drop-casting stands out for its straightforward nature, requiring less sophisticated equipment, as the solution is directly applied to the substrate and then dried either through heating or air drying [39]. Therefore, this study aims to compare the morphological, structural, and optical properties of ZnO nanorods (NRs) grown on ZnO-seeded PSi substrates through two unique techniques: drop-casting, which is an economical approach, and RF-sputtering, which is considered a more expensive technique. Additionally, the influence of each seeding method on the performance of MSM UV-ZnO NRs photodetectors will be examined.

Despite the importance of this comparative study, it appears that to my knowledge, there has been an absence of thorough research on this issue to date. However, drop-casting often results in uneven coverage on PSi substrates, failure to ensure seed solution enters deep into porous silicon, and heterogeneous distribution of ZnO seed solution between the pores and outer surface of pores, which leads to inconsistent and inhomogeneously growing ZnO NRs on and around pores.

To improve the seed layer distribution and growth of ZnO NRs for high-performance photodetector devices, the low-cost vibration-assisted drop-casting method (VADCM) is the best technique. VADCM ensures more uniform coverage across porous surfaces, reduces aggregation, and promotes consistent ZnO NRs growth, thereby enhancing the overall quality and performance of the fabricated photodetector devices. This is crucial, as a key challenge for optoelectronic devices in industry and marketing is lowering production costs. Therefore, finding inexpensive preparation techniques for nanomaterials is essential.

Developing photodetectors that can efficiently detect a broad spectrum of light, including UV, visible (Vis), and near-infrared (NIR) wavelengths, is crucial for various

technological applications such as communication, imaging, and environmental monitoring. Traditional photodetectors often suffer from limited spectral sensitivity and low responsivity, particularly in the NIR region. While ZnO nanorods exhibit excellent UV detection, their performance in visible and NIR ranges is limited due to their wide bandgap.

Integrating metal nanoparticles like Au and Ag with ZnO nanorods offers a promising solution to enhance these photodetectors' spectral sensitivity and responsivity across the UV-Vis-NIR range. The localized surface plasmon resonance (LSPR) effect of metal NPs can enhance light absorption, thereby improving the overall performance of photodetectors.

However, Limited research has investigated the plasmonic effects of noble metal nanoparticles (Au, Ag) synthesized via pulsed laser ablation in liquid (PLAL) on ZnO nanorods (NRs) grown on ZnO-seeded porous silicon (PSi) substrates prepared using the cost-effective VADCM. Furthermore, additional investigation is needed to assess the performance of MSM photodetectors based on the plasmonic effects of Au NPs, Ag NPs, and particularly their mixture (Au: Ag) NPs decorated on ZnO NRs/PSi substrates. This research will investigate how the NPs influence the operating range of the fabricated photodetectors across the UV-Vis-NIR spectrum, as previous studies on this specific topic are limited to our knowledge.

PSi provides a high surface area for efficient light absorption and charge carrier generation, which is advantageous for hybrid systems. Therefore, combining the unique properties of porous silicon with plasmonic nanostructures and organic materials led to the development and improvement of the performance of the photodetectors.

Combining inorganic elements like metal nanoparticles (such as Au or Ag) with organic materials (conductive polymers) allows the hybrid structure to take advantage of the nanoparticles' plasmonic effects and the organic layer's high optical absorption. These effects can lead to increased light absorption, improved charge separation, and enhanced photodetection sensitivity. Previous research has demonstrated that integrating noble and non-noble metal NPs, including Au NPs, Ag NPs, and others, into organic materials can significantly improve light absorption and charge transport, thereby enhancing the efficiency of solar cells [41, 42].

PEDOT: PSS, an organic material known for its moderate band gap, high conductivity, and broad absorption range extending to the infrared [36], has been extensively utilized in solar cells [43]. However, studies on the plasmonic effects influencing the performance of MSM photodetectors under UV-Vis-NIR light remain limited. Particularly research on fabricating such photodetectors using Au, Ag NPs, and specifically their mixtures decorated on ZnO NRs on porous silicon substrates.

Additionally, p-n heterojunction photodetectors (UV-Vis-NIR) based on Au NPs, Ag NPs, and specifically their mixtures embedded in PEDOT: PSS nanocomposites, deposited by a casting-hot air gun technique on n-PSi substrates, remain underexplored. On the other hand, the casting-hot air gun technique offers a simplified and cost-effective solution by directly casting the material onto the substrate and using a hot air gun for even distribution and setting. This method reduces equipment costs and processing time while improving uniformity in film deposition on Psi substrates, thus enhancing overall performance and efficiency.

This research aims to address this gap by exploring the incorporation of these noble metal NPs into PEDOT: PSS composites deposited by casting-hot air gun

technique on n-PSi to enhance photodetector applications. By leveraging the benefits observed in solar cell applications, this study seeks to improve photodetectors' efficiency, responsivity, and overall performance across a broad spectrum, thereby advancing the field and providing new insights into the role of metal NPs in organic-inorganic hybrid PDs.

1.3 Thesis Objectives

The major objectives of the current research are outlined as follows:

1. To evaluate the performance of UV MSM-ZnO NRs PDs fabricated on a ZnO-seeded PSi substrate using the vibration-assisted drop-casting method (VADCM) and RF-sputtering.
2. To fabricate (UV-Vis-NIR) MSM photodetectors using Au, Ag, and mixed NPs on ZnO NRs/PSi substrates and investigate their plasmonic effects on device performance.
3. To fabricate p-n heterojunction (UV-Vis-NIR) photodetectors using Au, Ag, and mixed NPs embedded in PEDOT: PSS nanocomposite on n-PSi substrates, and to study their plasmonic effects on hybrid device performance.
4. To demonstrate the effectiveness of cost-fabricated MSM and p-n hybrid photodetectors based on metal nanoparticles (Au, Ag, and their mixture) and PSi substrate for self-powered broadband (UV to NIR) detection.

1.4 Thesis Originality

The uniqueness of this research can be emphasized via several important aspects:

1. To the best of my knowledge, a comparison between the low-cost VADCM method and the more expensive RF-sputtering technique for fabricating ZnO-seeded PSi substrates has not previously been conducted for the production of high-performance MSM UV-ZnO NRs photodetectors.
2. Investigating the plasmonic effects of Au and Ag NPs, and especially their mixtures decorated on ZnO NRs/PSi substrate, on photodetector performance across a broad spectrum (UV-Vis-NIR) is a novel aspect that adds depth to the understanding of plasmonic-assisted photodetectors.
3. Exploring plasmonic effects in p-n heterojunction (UV–Vis-NIR) photodetectors based on Au NPs, Ag NPs, and their mixture embedded in PEDOT: PSS nanocomposite deposited by casting-hot air gun technique on n-PSi substrates significantly enhances the understanding of plasmonic-assisted photodetectors and advances the development of hybrid photodetector technology.
4. Using the cost-effective photodetector devices, such as MSM and p-n hybrid organic-inorganic structures based on a combination of metal nanoparticles (Au, Ag, and their mixture) and PSi substrates as ultra-high performance MSM-based self-powered PDs, which need more investigation.

1.5 Thesis Overview

This thesis comprises seven chapters and is organized in the following manner: The first chapter presents a concise introduction to ZnO nanostructures and the PEDOT: PSS polymer, including their importance, synthesis methods, and applications. It also discusses the significance of metal nanoparticles (Au, Ag NPs, and (Au: Ag) NPs) as decorations and nanocomposites for ZnO NRs and PEDOT: PSS, respectively. Furthermore, the chapter highlights the main problem of the study, the research objectives, and the originality aspect. Chapter 2 describes a comprehensive literature review concerning the fundamental properties of ZnO material and the PEDOT: PSS nanocomposite layer. It discusses the effect of metal NPs on ZnO NRs decorated using the UV photodeposition method and their impact on the PEDOT: PSS layer. This review covers MSM photodetectors, p-n heterojunction PDs, and their associated sensing mechanisms. Chapter 3 describes the synthesis methodologies, including the techniques and equipment for analyzing the synthesized materials and fabricating the MSM UV photodetectors and p-n heterojunction PDs. In Chapter 4, the characterization results are presented, along with a discussion comparing the performance of UV PDs fabricated using the cost-effective VADCM compared to those manufactured using the relatively higher-cost RF-sputtering method on Psi substrates. Chapter 5 discusses the results from the characterization of the fabrication of a UV-Vis-NIR photodetector using a hybrid structure of ZnO NRs decorated with Au, Ag NPs, and (Au: Ag) NPs on PSi substrates. Chapter 6 discusses on the fabrication of an organic-inorganic hybrid p-n heterojunction photodetector. Metal NPs and polymer nanocomposites have been employed in the fabrication of devices based on PSi substrates. Lastly, Chapter 7 summarizes the study's results and proposes directions for future research.

CHAPTER 2

REVIEW OF LITERATURE AND THEORETICAL FRAMEWORK

2.1 Introduction

In this chapter, the key properties of several nanomaterials, including Si nanostructures, ZnO materials, and noble metal nanoparticles (NPs) as well as the PEDOT: PSS polymer are presented. The synthesis methods of ZnO nanorods are described in general, specifically focusing on hydrothermal and chemical bath techniques and exploring the decoration of ZnO nanorods with nanoparticles for applications in MSM photodetectors. Furthermore, the chapter offers a comprehensive overview of MSM photodetectors and p-n heterojunctions, along with their sensing mechanisms. It includes essential mathematical formulations related to photoresponse characteristics. In addition, the chapter presents a comprehensive literature review and theoretical framework concerning noble metal-decorated ZnO nanorods and inorganic-PEDOT: PSS hybrids, particularly in the context of MSM photodetectors and hybrid organic-inorganic p-n heterojunction photodetectors.

2.2 General Properties of Silicon

Silicon (Si) is categorized within group 14 of the periodic table, alongside carbon (C), germanium (Ge), tin (Sn), and lead (Pb). It has an atomic number of 14 and an atomic mass of 28 [44]. As a tetravalent metalloid, silicon exhibits a unique combination of physical and chemical properties that render it suitable for a wide range of applications. Its characteristics reflect both metallic and non-metallic traits, which categorize it as a semiconductor material.

The doping process enables the adjustment of Si electrical conductivity by introducing impurities: n-type Si gains extra electrons, and p-type silicon has electron deficiencies, or "holes.". The interaction between n-type and p-type Si forms a p-n junction, a fundamental component essential for the operation of transistors and diodes [45]. Although pure Si acts as an insulator at room temperature, it transforms into a highly conductive material at elevated temperatures, particularly in high-temperature molten salt environments. The strong covalent bonds within Si lead to a diamond cubic lattice structure, contributing to its high melting point. The strong covalent bonds in silicon facilitate forming of a diamond cubic lattice structure, with each atom attached to four neighbours, thereby contributing to the material's high melting point.

Furthermore, Si electrical conductivity is not uniform across its various crystal faces; the [112] and [111] orientations demonstrate significant conductivity, whereas the [100] and [110] orientations exhibit reduced conductivity. The observed variation can be attributed to Si atoms' distinct orientations and arrangements, which affect electron movement and overall electrical behavior [45-48].

Crystal defects in Si, such as vacancies, interstitials, and dislocations, arise from impurities and lattice defects. The presence of these defects can have a considerable impact on the optical and electrical features of Si. In its bulk state, Si possesses a bandgap energy of 1.12 eV [46]. Si is widely used in photodetectors due to its favorable bandgap properties, making it a widely used semiconductor material. However, conventional Si-based photodetectors face challenges, including low detection in the UV spectrum and the need for anti-reflective coated glass substrates, leading to process complexity and high costs. To address these challenges, novel fabrication approaches involving nanostructured Si have been explored.

Nanostructured Si refers to Si materials with engineering properties at the nanoscale. These materials consist of minuscule structures formed from Si atoms. The exceptional features of these structures can be ascribed to their diverse shapes, sizes, small dimensions, and large surface area-to-volume ratios.

A variety of Si nanostructures can be identified, including nanowires, nanoparticles, quantum dots, and PSi. Specifically, nanowires are characterized as Si filaments with diameters varying from several tens to hundreds of nanometers, exhibiting a range of lengths. Nanoparticles are Si particles with dimensions in the nanoscale regime in all three dimensions. Quantum dots are zero-dimensional silicon structures where electrons are confined in all spatial directions, resembling nanoparticles but smaller in size. The PSi is characterized by a porous network throughout its structure, which is typically created through silicon etching techniques. This study utilized PSi as a nanostructure, generated through anodization and electrochemical etching techniques.

2.2.1 Background and Properties of Nanostructured Silicon

PSi is a material produced through the electrochemical etching process applied to a Si substrate. This process forms a network of interconnected Si nanocrystals with voids between them [15]. The accidental discovery of PSi can be traced back to the mid-1950s, when Arthur Uhriere Jr. and his wife, Ingeborg Uhriere, were attempting to electrochemically process silicon wafers at Bell Labs [13].

However, in the 1970s and 1980s, there was a notable increase in interest in PSi, which was largely due to its exceptionally high surface area, making it an important model for representing the crystalline Si surface in spectroscopic analyses. Additionally, PSi emerged as a precursor for generating thick oxide layers on Si and

served as a dielectric layer in capacitance-based chemical sensors [49]. In the year 1990s, Leigh Thomas Canham's research was pivotal in revitalizing interest in PSi. Canham's systematic investigation into its optical and electronic properties led to realising its potential applications in photonics, biosensing, and drug delivery [13, 50]. Detecting visible light emission from PSi has prompted extensive research into its potential optoelectronic applications.

The PSi has been extensively investigated in the last twenty years due to its exceptional optical properties, mechanical robustness, thermal stability, strong matches with Si-based technologies, and inexpensive. Its unique characteristics, including large surface area, tunable pore sizes, favorable surface chemistry, and controllable refractive index, have positioned porous silicon as a versatile material for constructing advanced optoelectronic devices and multilayered structures [49]. PSi is highly regarded in developing optoelectronic devices due to its distinctive properties, including excellent light absorption, a tunable band gap, and a large surface-to-volume ratio.

Moreover, PSi offers cost-effective fabrication and exhibits high optical gain while maintaining a similar crystal structure to standard crystalline bulk silicon. Additionally, its optical characteristics, such as photoluminescence and quantum confinement effects, can be fine-tuned by controlling the shapes, density, and dimensions of the pores [50].

PSi is fabrication using two major approaches: the top-down and bottom-up methods. In the top-down method, Si atoms are removed from a substrate to create voids, while the bottom-up approach involves assembling Si clusters to form a porous structure [51]. Electrochemical etching is a commonly utilized method for producing

PSi, as it allows the precise regulation of pore formation through adjustments in current density. It provides reproducibility and the ability to adjust the geometry and architecture of PSi [15, 51, 52].

The optical characteristics of PSi are significantly influenced by the dimensions of its pores. This variation in pore size leads to alterations in both absorption and emission spectra; specifically, smaller pore sizes tend to cause a movement towards shorter wavelengths, of the absorption and emission peaks. Additionally, this decrease in pore size is associated with an expansion in the refractive index and enhanced light scattering. This allows PSi to operate across the spectrum of wavelengths, including the infrared, visible, and UV regions. The specific working wavelength range depends on the fabrication parameters and porosity level [53, 54].

Pore sizes in PSi can be categorized into groups such as macropores (greater than 50 nm), mesopores (ranging from 2 to 50 nm), and micropores (less than 2 nm). This classification is important as it determines the optical behavior of PSi and other relevant characteristics. By controlling the pore size, the optical features of PSi can be finely changed, making it promising for applications in optoelectronic devices and sensor technologies [15-17].

Furthermore, PSi exhibits a tunable band gap that can be modified by regulating the fabrication parameters and porosity level. PSi also exhibits strong photoluminescence, with emission peaks ranging from the red to the near-infrared region. The properties of this emission can be adjusted by controlling the fabrication parameters and implementing surface passivation techniques [55]. H. Chen and F. Chen demonstrated that the etching of n-type PSi presents challenges due to the necessity of holes to drive the reaction forward [56]. To address this issue, they

illuminated the sample using a 60 W bulb, thereby promoting the generation of hole carriers to facilitate the etching process.

2.2.2 Formation Mechanism of Porous Silicon

The formation of a porous structure in n-type Si begins with the activation of electrons due to exposure to light, which induces a photocurrent and enables electron injection into the Si substrate. Following this, chemical interactions occur between the injected electrons and fluoride ions (F-) present in the HF electrolyte solution. These interactions drive the dissolution of Si, resulting in the fabrication of porous structures within the material.

When an n-type Si substrate is illuminated, photons energize electrons, prompting their transition from the valence band to the conduction band within the material. This excitation process generates a photocurrent as excited electrons accumulate within the material [57]. Initially, the surface of Si atoms is passivated by forming bonds with hydrogen atoms (Si-H bonds) (1). Subsequently, holes are introduced from the bulk into the Si surface via an external power supply. Fluoride ions (F-) can then nucleophilically attack the Si-H bonds, forming Si-F bonds (2). Si-F bonds induce a polarisation effect, permitting additional fluoride ions to interchange the remaining hydrogen bonds (3) [51]. Consequently, two hydrogen atoms merge, resulting in the injection of an electron into the substrate. The induced polarisation by Si-F bonds decreases the electron density of the residual Si-Si bonds, rendering them more reactive towards hydrofluoric acid (HF). This ongoing reaction ultimately yields Si tetrafluoride (SiF_4) (4), as the remaining surface Si atoms bond with hydrogen atoms. These hydrogen atoms undergo a subsequent nucleophilic attack by fluoride ions, culminating in the formation of SiF_4. After that, the SiF_4 molecule reacts with HF

to make the very stable SiF_6^{-2} (silicon hexafluoride ion). The surface returns to a neutral state until another hole opens [51, 58]. The reactions during the pore formation are written as follows [59, 60]:

$$Si + 6HF \rightarrow H_2SiF_6 + H_2 + 2H^+ + 2e^- \quad (2.1)$$

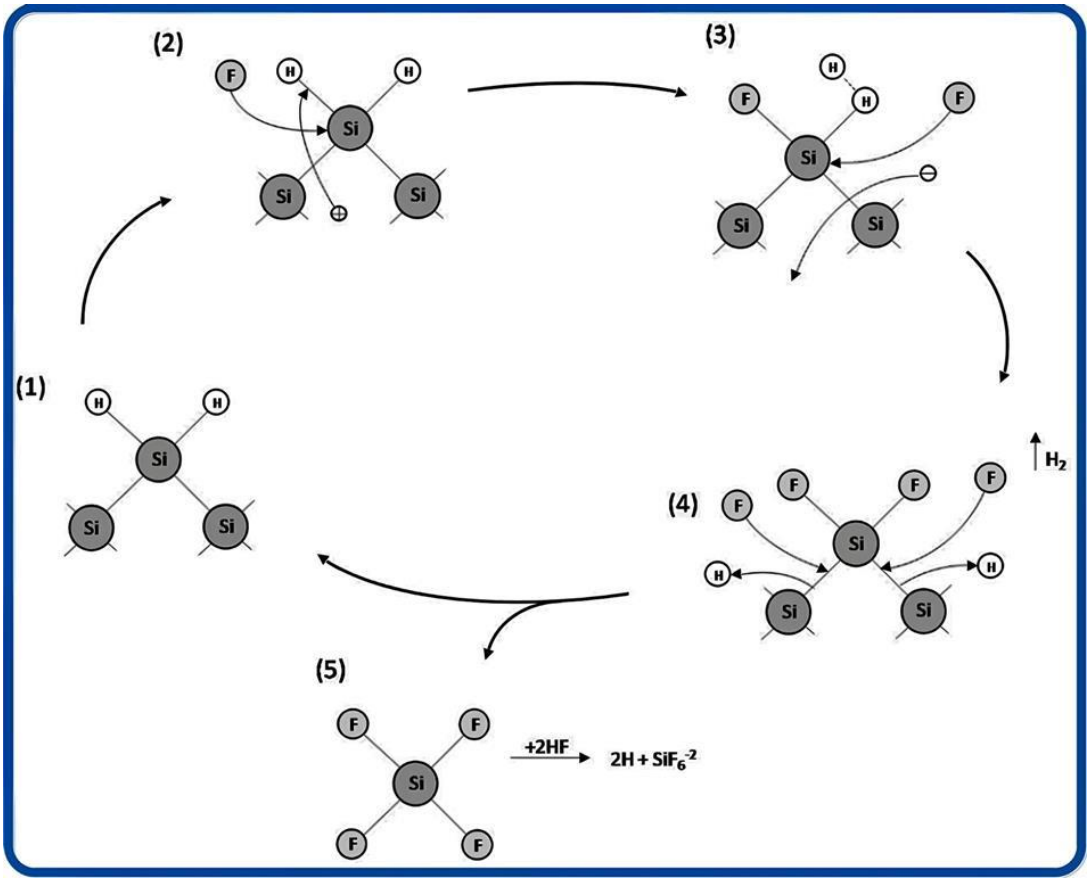

Figure 2.1 Schematic illustration of the growth mechanism of porous silicon [58].

2.3 General Features of ZnO

ZnO is a widely studied inorganic substance renowned for its white, powdery appearance and its insolubility in water. It is comprised of zinc (Zn) and oxygen (O), and it is abundantly available within the earth's crust [61]. At different conditions, zinc oxide (ZnO) can crystallize in various structures. Under standard atmospheric pressure, it typically adopts the hexagonal wurtzite configuration. However, when

grown on a cubic substrate like ZnS, it can take on the zincblende structure, and under certain circumstances, it may exhibit the rock salt (NaCl) structure [62]. Figure 2.1 illustrates various crystal structures, such as Wurtzite, Zinc blende, and Rock salt.

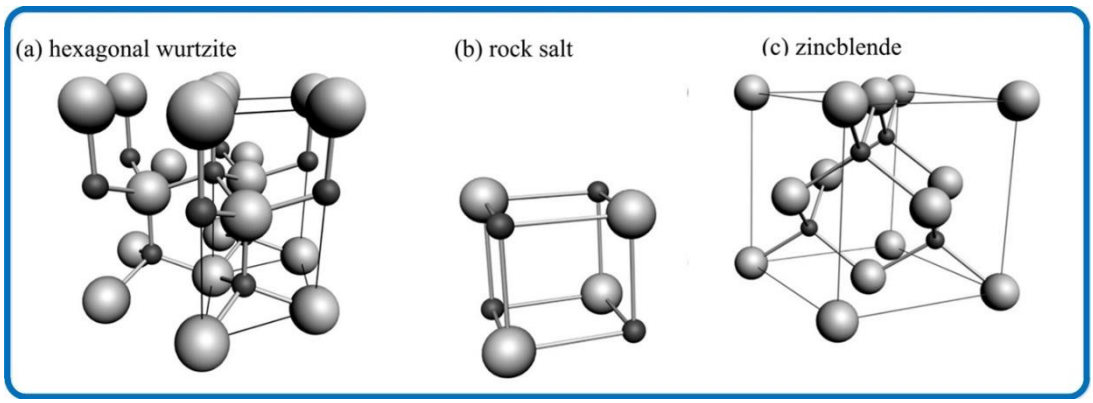

Figure 2.2 Visualization of ZnO crystal structures: (a) hexagonal wurtzite, (b) cubic rock salt, (c) cubic zincblende. Oxygen atoms are depicted as large white spheres, while Zinc atoms are represented as smaller black spheres [63].

2.3.1 Crystal Structure of ZnO

The hexagonal lattice arrangement characterizes the wurtzite structure of ZnO, with zinc (Zn^{2+}) and oxygen (O^{2-}) ions forming interconnected sublattices. The tetrahedral arrangement of O ions surrounding each Zn ion, and vice versa, gives ZnO a polar symmetry along its hexagonal axis. This inherent polarity is responsible for ZnO's piezoelectric and spontaneous polarization properties, and significantly impacts its crystal growth, etching, and defect formation processes [64, 65]. The hexagonal unit cell of ZnO has lattice parameters of a = 3.2495 Å and c = 5.2069 Å, with a density of 5.605 g/cm³.

2.3.2 Optical Properties of ZnO

ZnO stands out for its remarkable properties, including a large direct band gap of 3.37 eV, and a high exciton binding energy of 60 meV at room temperature, making it a highly promising material for various nanotechnology applications [66, 67]. These

applications range from UV detectors and photocatalysis to chemical sensors, biosensors, thermal imaging, solar cells, ultraviolet laser diodes, and cancer treatment [40, 68].

Direct bandgap materials like ZnO typically exhibit superior luminescence compared to indirect bandgap materials, while wide bandgap materials also help reduce device leakage current. Furthermore, absorption spectroscopy and photoluminescence (PL) analysis are often employed to examine the optical features of crystalline ZnO. As reported in the literature, the quality of crystals and the accumulation of defects or impurities significantly influence the optical properties of oxide nanostructures [69, 70]. ZnO nanostructures exhibit strong absorbance in the UV-Vis region, particularly at shorter wavelengths below 380 nm in the UV range. This signifies their capability for effective light absorption in the UV. Conversely, the absorption characteristics of ZnO nanostructures reveal considerable transparency in the visible spectrum and at longer wavelengths above 380 nm, indicating that ZnO allows light to pass through these regions [71, 72].

PL spectra commonly exhibit a UV emission peak at around 378 nm (3.28 eV), corresponding to near-band edge (NBE) emission from free exciton recombination. This emission is crucial for numerous applications, such as UV light-emitting diodes (LEDs). Conversely, broad visible peaks, termed deep-level emissions (DLE), are typically observed between 400 and 720 nm, originating from native defects within the material [73]. However, the exact origins of these DLEs remain incompletely understood, with proposed explanations including oxygen and zinc vacancies or interstitial oxygen and interstitial zinc [74, 75].

The theoretical calculations indicate the energy levels associated with defects in ZnO, with specific positions relative to the conduction band: Zinc vacancies (V_{Zn}) are estimated to be situated 3.06 eV beneath the conduction band, while oxygen vacancies (V_o) are found at a depth of 2.47 eV below the conduction band. Furthermore, zinc interstitial defects are identified at 0.22 eV below the conduction band. Oxygen interstitial defects lie at 2.28 eV below the conduction band [75]. A band diagram illustrating the DLE emission in ZnO (Figure 2.3) demonstrates the recombination of electron-hole pairs originating from various defects into the valence band, resulting in photon emission. The defect density and quality assessment of ZnO materials depend significantly on the ratio of ultraviolet emission intensity to deep visible level intensity (I_{UV}/I_{DLE}). A pronounced disparity in intensity signifies the presence of high-quality ZnO nanowires characterized by a well-defined hexagonal structure [76, 77].

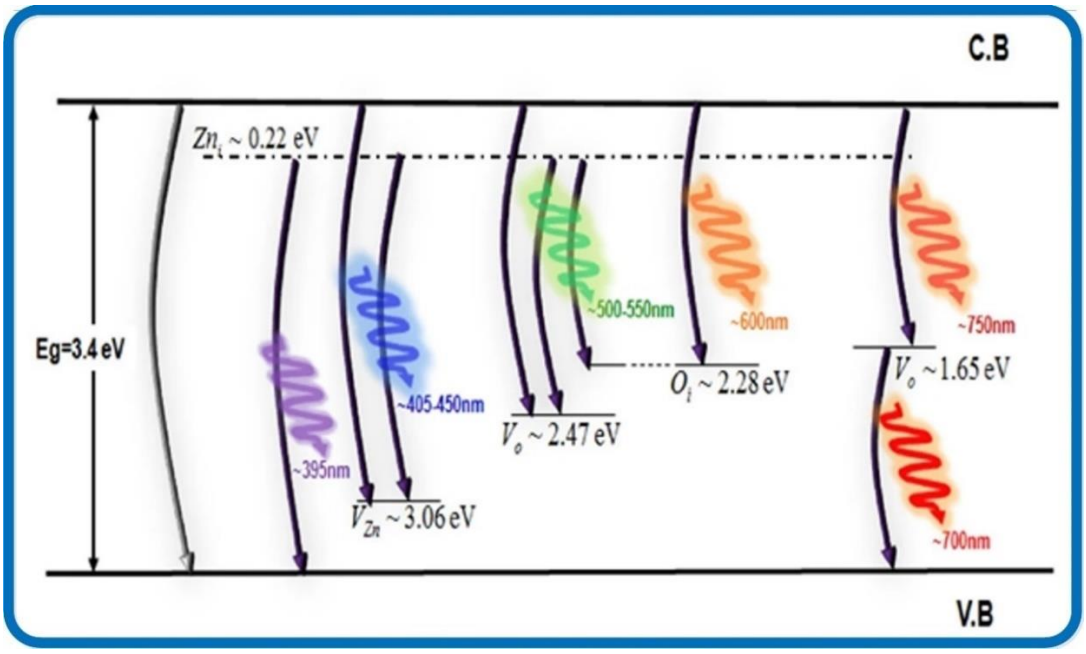

Figure 2.3 Schematic energy level diagram of various defect level emissions in ZnO [78].

2.3.3 Growth Methods of ZnO Seed Layer

Various deposition techniques have recently been employed to produce c-axis-textured ZnO seed layers, including the electrospray laser chemical vapor deposition method [79], atomic-layer additive manufacturing (ALAM) [80], ALD [81], CVD [82] PLD [82], sol-gel spin coating process [83], printing technologies like inkjet and gravure printing [84], MOCVD [85], chemical spray pyrolysis [86], magnetron sputtering [87, 88], drop-casting [89], and PVD [54]. A physical vapor deposition (PVD) technique, is highly effective for epitaxial growth of semiconductors on various substrates, including Si wafers. It can successfully sputter high melting point materials that are difficult to evaporate. The sputter-deposited films closely match the target composition and exhibit excellent adhesion, making them suitable for device applications.

In 1933, Robertson and Clapp made the initial observation of radio frequency (RF) discharge during the sputtering process [90]. By the 1960s, RF sputtering had been employed for the sputtering of dielectric thin films [91]. RF sputtering systems can operate at lower pressures (around 1 mTorr) while sustaining a glow discharge, playing a vital role in depositing high-quality thin films. However, both DC and RF sputtering processes are limited by low deposition rates, low plasma ionization efficiencies, and significant substrate heating effects [92]. Magnetron sputtering overcomes these limitations by using magnetic fields to confine the plasma near the target, enhancing ion bombardment. First proposed by Frans in 1936 (Coating by cathode disintegration), magnetron sputtering studied low-pressure sputtering with a transverse magnetic field superimposed on a DC plasma tube. This method allows for the deposition of thicker films compared to DC and RF sputtering, with low-pressure conditions reducing contamination and achieving high deposition rates. Magnetron

sputtering is widely used for the deposition of high-quality thin films and coatings, owing to its versatility and capacity to produce uniform, well-adhered films on various substrates.

Notably, drop-casting has emerged as an exceptionally straightforward method due to its simple solution deposition process onto a substrate followed by drying, either through heating or air drying. One simple example of this method is using zinc acetate dihydrate (ZAD), which undergoes a reaction with ethanol to produce ZnO seed layers [18]. This method represents a clear and effective strategy for developing seed layers. Greene et al. [18] were pioneers in reporting the application of ZAD as a seed layer, demonstrating that thermal degradation of ZAD in 98% ethanol at 200-350 °C results in the formation of a c-axis oriented ZnO nanocrystalline thin layer across various substrates.

Drop casting presents a straightforward and cost-effective approach for depositing seed layers in the fabrication process of ZnO nanostructures. This method facilitates the enhancement of crystallinity and orientation in ZnO films, resulting in improved device performance, particularly UV photodetectors. Enhancing the seed layer for ZnO films can improve the orientation and adhesion, increase the growth rate, and improve the film quality [93]. These enhancements are vital factors that influence the overall performance of devices, particularly in terms of their optical and electrical features, ultimately contributing to the efficiency and sensitivity of UV photodetectors. Drop casting helps ZnO nanorods grow vertically by letting oriented seed layers be deposited at room temperature [94].

Additionally, the drop-casting method can be used to synthesize ZnO seed layers on various substrates, including FTO (Fluorine-doped Tin Oxide) glass, silicon,

ITO/PES (Indium Tin Oxide-coated Polyethersulfone), and porous silicon. Research communities have found this method very important, as it enables them to produce high-quality seed layers of ZnO film [83]. ZnO NRs will grow more densely, fully aligned, and highly quality if the film is seeded with high-quality seed layers [95]. These nanorods demonstrate the important roles of ZnO in UV detectors [39].

Suhail et al. [96], fabricated ZnO nanofilms via the chemical spray pyrolysis technique. A 0.1 M spray solution was prepared by dissolving ZAD (Zn $(CH_3COO)_2(H_2O)_2$) with a molarity of 0.1 M and a molecular weight of 219.49 g/mol in distilled water. The solution was then atomized and sprayed onto preheated substrates using pressurized nitrogen gas flow. The films were deposited onto a PSi layer heated to 400 °C. The duration of each spraying cycle was 4 seconds, regulated by an adjustable solenoid valve, succeeded by a 12-second interval to facilitate the drying of the deposited ZnO layer. The ideal experimental conditions for producing a homogeneous ZnO thin film at a temperature of 400 °C were established by considering factors such as gas pressure, spraying duration, and drying duration. This approach allowed for the fabrication of ZnO films with a thickness approximately equal to 1 μm.

Ameer Azam and Saeed Salem Babkai [95] developed a seed layer for subsequent nanorod growth, employing ZnO nanocrystals synthesized via the acetate route. The Si substrate underwent ultrasonic cleaning in acetone and deionized (DI) water to eliminate impurities and oxide layers. In the synthesis process, a solution of 20 mM ZAD (Zn $(CH_3COO)_2$ $2H_2O$) and 10 mM sodium hydroxide (NaOH) in ethanol was stirred at 70 °C for 2 hours, yielding a white ZnO seed suspension. This suspension was then drop-cast on the Si substrate and then dried at 200 °C for 1 hour to ensure optimal adhesion of the seed particles to the substrate.